

Full paper / Mémoire

Cyanido-bridged bimetallic two-dimensional network based on dinuclear manganese(III) Schiff base complex and hexacyanochromate(III) building block

Xueting Liu^{a,b}, Olivier Roubeau^{a,b}, Rodolphe Clérac^{a,b,*}

^a CNRS, UPR 8641, Centre de Recherche Paul Pascal (CRPP), Equipe “Matériaux Moléculaires Magnétiques”,
115 avenue du Dr. Albert Schweitzer, Pessac, 33600, France

^b Université de Bordeaux, UPR 8641, Pessac, 33600, France

Received 30 January 2008; accepted after revision 7 April 2008

Available online 26 July 2008

Abstract

Reaction between the dimeric $[\text{Mn}_2(\text{saltmen})_2(\text{H}_2\text{O})_2]^{2+}$ cations (with saltmen = *N,N'*-(1,1,2,2-tetraméthyléthylène)bis(salicylidèneiminato) dianion) and $[\text{Cr}(\text{CN})_6]^{3-}$ anions results in the isolation of a 2D layered complex, $[\{\text{Mn}(\text{saltmen})\}_4\text{Cr}(\text{CN})_6]\text{ClO}_4$ (**1**), whose crystal structure has been determined and presents pentameric cyanido-bridged CrMn_4 units assembled into extended layers through saltmen phenoxo Mn–Mn bridges. Detailed magnetic measurements and their analysis show that the layers have a ferrimagnetic organization with antiferromagnetic exchange coupling ($J/k_B = -7(1)$ K) between Mn(III) and Cr(III) ions through cyanide bridges and ferromagnetic interaction between Mn(III) ions through phenoxo bridges. Compound **1** displays a glassy ferrimagnetic ordering with $T_C = 5$ K. Magneto-structural discussions for **1** and three similar 2D systems are developed that explain the antiferromagnetic coupling observed in the cyanido-bridged Mn(III)–Cr(III) cases. **To cite this article:** X. Liu *et al.*, *C. R. Chimie 11 (2008)*.

© 2008 Académie des sciences. Published by Elsevier Masson SAS. All rights reserved.

Résumé

La réaction entre le cation $[\text{Mn}_2(\text{saltmen})_2(\text{H}_2\text{O})_2]^{2+}$ (avec saltmen = dianion *N,N'*-(1,1,2,2-tétraméthyléthylène)bis(salicylidèneiminato)) et l'anion $[\text{Cr}(\text{CN})_6]^{3-}$ produit un complexe bidimensionnel, $[\{\text{Mn}(\text{saltmen})\}_4\text{Cr}(\text{CN})_6]\text{ClO}_4$ (**1**), dont la structure cristalline a été déterminée et est constituée d'unités pentamériques $[\text{CrMn}_4]$ assemblées en couches par le biais de ponts Mn–Mn à travers les fonctions phénolate du ligand saltmen. Des mesures magnétiques détaillées et leur analyse montrent que les couches présentent une organisation ferrimagnétique des sites magnétiques, les couplages à travers les ponts cyanuro (Cr(III)–CN–Mn(III)) et phénolate (Mn(III)–O₂–Mn(III)) étant respectivement antiferromagnétique ($J/k_B = -7$ K) et faiblement ferromagnétique. Le composé **1** présente un ordre ferrimagnétique à caractère vitreux aux alentours de 5 K. Des considérations magnéto-structurales sur le composé **1** et trois systèmes 2D analogues permettent de comprendre le couplage

* Corresponding author. CNRS, UPR 8641, Centre de Recherche Paul Pascal (CRPP), Equipe “Matériaux Moléculaires Magnétiques”, 115 avenue du Dr. Albert Schweitzer, Pessac, 33600, France.

E-mail address: clerac@crpp-bordeaux.cnrs.fr (R. Clérac).

antiferromagnétique observé à travers le pont cyanuro dans les cas Mn(III)–Cr(III). *Pour citer cet article* : X. Liu et al., C. R. Chimie 11 (2008).

© 2008 Académie des sciences. Published by Elsevier Masson SAS. All rights reserved.

Keywords: Cyanide ligands; Magnetic properties; Chromium; Manganese; Schiff-base ligands

Mots-clés : Ligand cyanure ; Propriétés magnétiques ; Chrome ; Manganèse ; Base de Schiff

1. Introduction

The field of molecular magnetism [1] continues to depend largely on the use of chelating–bridging polydentate ligands that possess the coordination abilities to direct the formation of discrete high-nuclearity complexes and to assemble precursor building blocks into higher dimensionality systems. Indeed, discrete complexes with a combination of sufficient high-spin ground state (S_T) and uni-axial anisotropy (D) have been one of the main areas in this field of research in the past two decades as they may exhibit Single-Molecule Magnet (SMM) properties i.e. slow dynamics of their magnetization [2]. On the other hand, the assembly of magnetic building blocks into extended bi- (2D) or tri-dimensional (3D) coordination networks has been used to obtain classical magnets, in certain cases of high critical temperatures [3]. More recently, one-dimensional (1D) systems have been shown to potentially present slow relaxation of the magnetization [4–9]. In these materials, called single-chain magnets (SCMs) [5], the slow relaxation of magnetization depends on the magnetic correlations (J) along the chain, although a high-spin ground state (S_T) and uni-axial anisotropy (D) of each spin unit composing the chain remain essential ingredients to obtain this property [6]. More generally, these compounds are 1D assemblies of spins (metal ions, organic radicals or metal–ion complexes) that can be coupled ferro- [5,7,8] or antiferromagnetically [4]. The latter case corresponds to systems with a non-compensation of spins along the chain (ferrimagnetic or canted-antiferromagnetic arrangements) [4]. In all these cases i.e. SMMs, classical magnets or SCMs, the hexacyanometalate $[M(CN)_6]^{n-}$ building block, which acts as a cyanide donor ligand to coordinate another $[M'(L)]^{m+}$ acceptor complex has been widely used to form a bimetallic assembly, resulting in the synthesis of high T_C molecule-based magnets with long-range magnetic ordering [10], SMMs [11], photomagnetic molecular or molecule-based materials [12], etc. On the other hand, Mn(III) Schiff base

complexes, $[Mn(L)]^+$ (where L = tetradentate ligand), featuring a high-spin ground state and strong uni-axial anisotropy induced by the Jahn–Teller distortion of Mn(III) ion in an octahedral ligand field, have shown great versatility to obtain SMM [13] and SCM [5] systems. Therefore the combination of hexacyanometalate and Mn(III) Schiff base complex building blocks seems a promising strategy that has already produced a great number of bimetallic complexes with polynuclear [14], 1D [5] and 2D [15] structures with remarkable magnetic behaviors. In our efforts towards the design of new SCMs based on hexacyanometalate, we have isolated a new 2D bimetallic system, $[Mn(\text{saltmen})_4Cr(CN)_6]ClO_4$ (**1**), obtained by the assembly of $[Mn(\text{saltmen})]^+$ and $[Cr(CN)_6]^{3-}$ building blocks (saltmen = N,N' -(1,1,2,2-tetramethylene)bis(salicylideneiminato) dianion). We report here its synthesis and crystal structure, together with magnetic studies indicating the presence of a long-range magnetic order at low temperature that will be compared with known related 2D systems.

Table 1
Crystal data of $[Mn(\text{saltmen})_4Cr(CN)_6]ClO_4$

Empirical formula	$C_{172}H_{176}Cl_2Cr_2Mn_8N_{28}O_{24}$
Formula weight	3633.83
Temperature (K)	150(2)
Wavelength	0.71073 Å
Crystal size	0.22 × 0.20 × 0.07 mm ³
Crystal system, space group	Tetragonal, $I4/m$
Unit cell dimensions	$a = 18.706(2)$ Å, $\alpha = 90.00^\circ$ $b = 18.706(2)$ Å, $\beta = 90.00^\circ$ $c = 28.268(5)$ Å, $\gamma = 90.00^\circ$
Volume	9891(2) Å ³
Z	2
Absorption coefficient	0.689 mm ⁻¹
$F(000)$	3756
Max. and min. transmission	0.95 and 0.86
Data/restraints/parameters	3084/34/286
Final R indices [$I > 2\sigma(I)$]	$R_1 = 0.0872$, $wR_2 = 0.2363$
R indices (all data)	$R_1 = 0.1295$, $wR_2 = 0.2725$
Goodness-of-fit on F^2	1.084
Largest diff. peak and hole	0.783 and -0.455 e Å ⁻³

2. Experimental section

2.1. Materials

All chemicals and solvents used in the synthesis were of reagent grade. The precursor, $[\text{Mn}_2(\text{saltmen})_2(\text{H}_2\text{O})_2](\text{ClO}_4)_2$, was prepared according to the literature procedure [16]. *Caution: perchlorate salts of metal complexes with organic ligands are potentially explosive. Only a small amount of the material should be prepared and it should be handled with extreme care.*

2.2. Physical measurements

FTIR spectra were recorded in the range of 400–4000 cm^{-1} on a Nicolet 750 Magna-IR spectrometer using KBr pellets. Magnetic susceptibility measurements were obtained with the use of a Quantum Design SQUID magnetometer (MPMS-XL). dc measurements were conducted from 1.8 to 300 K and from –70 kOe to 70 kOe. The measurements were performed on a polycrystalline sample. Experimental data were corrected for the sample holder and for the diamagnetic contribution of the sample. *Crystallography*: X-ray crystallographic data were collected on a Nonius Kappa CCD diffractometer with a graphite-monochromated Mo $K\alpha$ radiation ($\lambda = 0.71073 \text{ \AA}$) at 150 K. A suitable crystal was affixed to the end of a glass fiber using silicone grease and transferred to the goniostat. DENZO-SMN [17] was used for data integration and SCALEPACK [17] corrected data for Lorentz-polarisation effects. The structure was solved by direct methods and refined by a full-matrix least-squares method on F^2 using the SHELXTL crystallographic software package [18]. Crystal data of **1** are summarized in (Table 1).

2.3. Synthesis of $[\{\text{Mn}(\text{saltmen})\}_4\text{Cr}(\text{CN})_6]\text{ClO}_4$

The synthetic process was carried out in the dark to avoid decomposition of $\text{K}_3[\text{Cr}(\text{CN})_6]$. $[\text{Mn}_2(\text{saltmen})_2(\text{H}_2\text{O})_2](\text{ClO}_4)_2$ (0.2 mmol, 0.1908 g) in methanol was mixed with $\text{K}_3[\text{Cr}(\text{CN})_6]$ (0.2 mmol, 0.0650 g) in H_2O . A precipitate formed after about one week. This solid was then dissolved in warm H_2O /methanol mixture and the resulting black solution filtered. The filtrate was left undisturbed to produce brown plate-like crystals suitable for X-ray diffraction within a few days. These crystals were collected by filtration, washed with 1:1 (v/v) water/methanol, and dried in air at room temperature. Yield: 0.128 g (35% based on Cr). IR (KBr, cm^{-1}): 3425.3 (br, m), 2981.9 (w), 2141.4 (m), 1602.3 (vs), 1542.2 (vs), 1468.8 (m), 1443.9 (s), 1394.4 (s), 1302.6 (s), 1210.9

(w), 1144.6 (s), 1126.2 (m), 1095.7 (br, s), 958.6 (w), 907.0 (w), 848.0 (w), 798.7 (w), 950.8 (s), 628.0 (s), 534.8 (m), 456.6 (m), 429.4 (w).

3. Results and discussion

3.1. Synthesis and structure of **1**

While one-dimensional architectures were targeted in this work, the reactions between hexacyanochromate precursor and $[\text{Mn}_2(\text{saltmen})_2(\text{H}_2\text{O})_2](\text{ClO}_4)_2$ in various ratios reproductively led to brown crystals of $[\{\text{Mn}(\text{saltmen})\}_4\text{Cr}(\text{CN})_6](\text{ClO}_4)$ (**1**) that exhibited an extended 2D network. This result illustrates that a simple stoichiometry-based strategy to control the architecture of a given system is not in most of cases sufficient and requires the use of designed building blocks with coordination sites selectively blocked by polydentate chelating ligands [12a]. Complex **1** consists of pentanuclear $[\{\text{Mn}(\text{saltmen})\}_4\text{Cr}(\text{CN})_6]^+$ unit and a perchlorate counter ion (Fig. 1). Selected bond distances and angles for **1** are listed in Table 2.

The Cr^{III} ion in the pentanuclear unit is coordinated via four cyanido bridges to four symmetry-related Mn^{III} ions with the C5–N6–Mn2 bond angle of $156.2(6)^\circ$. This geometric parameter is very similar to the one found in the three analogue compounds: $[\{\text{Mn}(\text{saltmen})\}_4\text{Cr}(\text{CN})_5(\text{NO})]\text{ClO}_4 \cdot 3\text{H}_2\text{O}$ [19], $[\{\text{Mn}(\text{saltmen})\}_4\{\text{Fe}(\text{CN})_6\}]\text{ClO}_4 \cdot \text{H}_2\text{O}$ [15a] and $[\{\text{Mn}(\text{saltmen})\}_4\{\text{Fe}(\text{CN})_5(1 - \text{CH}_3\text{im})\}_n][\text{ClO}_4]_{2n} \cdot 9n\text{H}_2\text{O}$ [20] where the corresponding angles are $154.6(8)^\circ$, 156.1

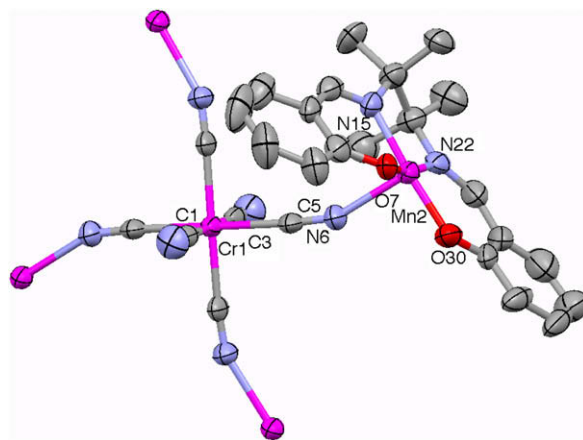


Fig. 1. ORTEP view of the pentanuclear unit $[\{\text{Mn}(\text{saltmen})\}_4\text{Cr}(\text{CN})_6]^+$ in **1**. For clarity, only one of the four symmetry-equivalent saltmen ligands is depicted, and the perchlorate anion and H atoms are omitted. Ellipsoids are drawn at 50% probability. Colour code: Cr and Mn, purple; N, blue; C, grey; O, red. For interpretation of the references to colour in this figure legend, the reader is referred to the web version of this article.

(10° and 157.3(7)°, respectively). Each pentanuclear motif is then connected to four other adjacent units via the out-of-plane bi-phenoxo bridges forming the well-known dimeric $[\text{Mn}(\text{saltmen})_2]^{2+}$ cation [9,16] to give the 2D network structure (Fig. 2). The Mn^{III} ion has a distorted octahedral geometry with equatorial plane occupied by O_2N_2 donor atoms from tetradentate Schiff base ligand (saltmen), and axial positions occupied by one N atom from cyanide bridge and one phenolate oxygen atom from a $[\text{Mn}(\text{saltmen})]^{+}$ cation of an adjacent pentanuclear unit. Due to the Jahn–Teller distortion of the Mn^{III} ion, its two axial bond lengths, 2.205(7) Å ($\text{Mn}-\text{N}_{\text{cyanido}}$) and 2.607 Å ($\text{Mn}-\text{O}_{\text{phenoxo}}$), are relatively longer than those of its equatorial bond lengths (between 1.876 Å and 1.890 Å), but comparable

to those of $[\{\text{Mn}(\text{saltmen})\}_4\text{Cr}(\text{CN})_5(\text{NO})]\text{ClO}_4 \cdot 3\text{H}_2\text{O}$ (2.166(9) Å and 2.629(11) Å), $[\{\text{Mn}(\text{saltmen})\}_4\{\text{Fe}(\text{CN})_6\}]\text{ClO}_4 \cdot \text{H}_2\text{O}$ (2.19(1) Å and 2.847(9) Å) and $[\{\text{Mn}(\text{saltmen})\}_4\text{Fe}(\text{CN})_5(1-\text{CH}_3\text{im})](\text{ClO}_4)_2 \cdot 9\text{H}_2\text{O}$ (2.197(8) Å and 2.844(8) Å) [15a,19,20]. The $\text{Mn}\cdots\text{Cr}$ distance in the $[\text{Mn}_4\text{Cr}]$ unit is 5.280 Å, while the $\text{Mn}\cdots\text{Mn}$ distance in the Mn dimer is 3.480 Å. As shown in Fig. 3, which presents a view of the stacking of layers in **1**, the 2D sheets are well separated by the ClO_4^- anions.

3.2. Magnetic properties of **1**

The magnetic susceptibility of **1** was measured in the temperature range of 1.8–300 K under an applied

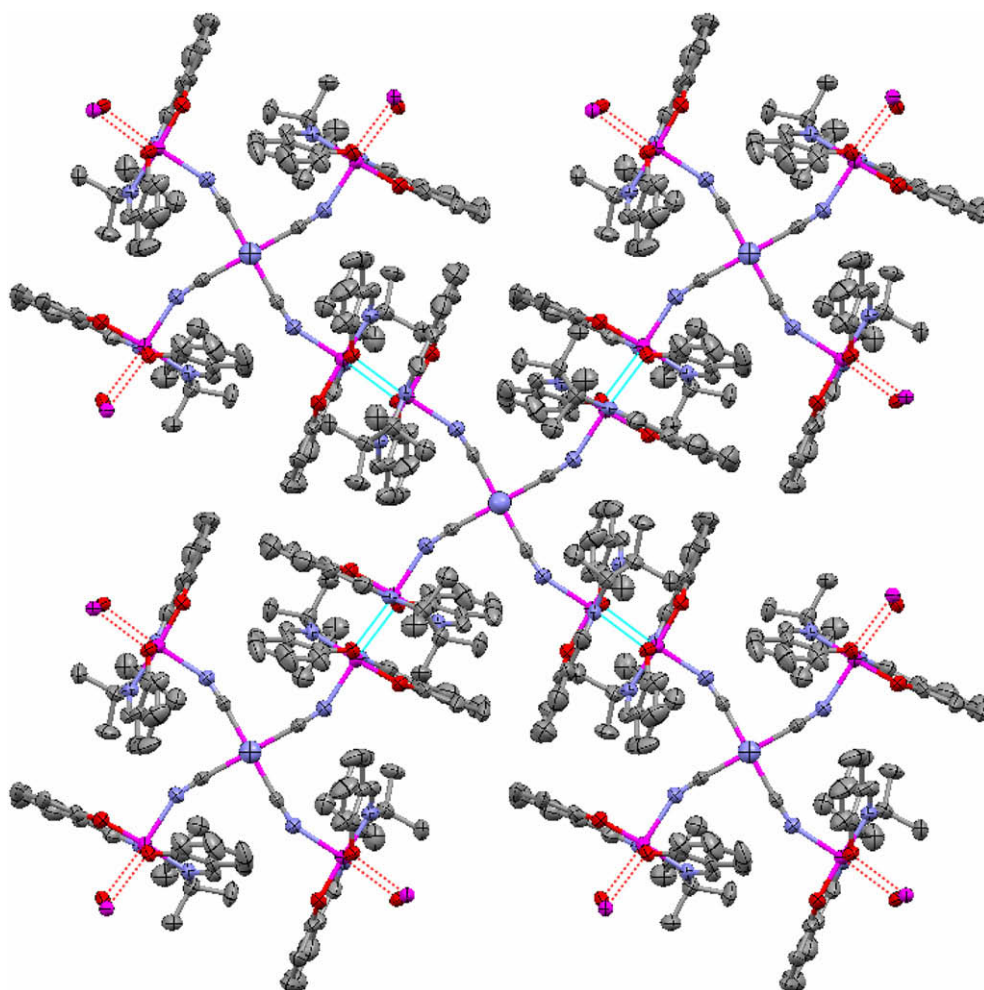


Fig. 2. A view along the crystallographic c axis showing the 2D network structure in **1** constructed by out-of-plane double phenoxo bridges (see the dotted blue and red lines) between $[\text{Mn}(\text{saltmen})]^{+}$ ions. Perchlorate anions and H atoms are omitted for clarity. Colour code: Cr and Mn, purple; N, blue; C, grey; O, red. For interpretation of the references to colour in this figure legend, the reader is referred to the web version of this article.

Table 2
Selected bond lengths [\AA] and angles [$^\circ$] in **1**

Cr1–C3	1.99(3)	C1–Cr1–C5	91.4(3)
Cr1–C1	2.06(2)	N2–C1–Cr1	180
Cr1–C5	2.068(9)	N4–C3–Cr1	180
Mn2–N22	1.954(8)	C5–N6–Mn2	156.2(6)
Mn2–O7	1.876(6)	O7–Mn2–N6	92.3(2)
Mn2–O30	1.882(5)	O30–Mn2–N6	93.4(2)
Mn2–N15	1.980(7)	N22–Mn2–N6	98.3(3)
Mn2–N6	2.205(7)	N15–Mn2–N6	89.5(2)
C3–Cr1–C1	180	N6–C5–Cr1	174.7(7)
C3–Cr1–C5	88.6(3)		

magnetic field of 1000 Oe. The plot of χT vs T is shown in Fig. 4, where χ is the magnetic susceptibility (M/H) per Mn_4Cr unit. At room temperature, the χT product is $12.8 \text{ cm}^3 \text{ K/mol}$. As expected when antiferromagnetic interactions are present (vide infra), this value is slightly lower than the spin-only value ($13.875 \text{ cm}^3 \text{ K/mol}$ with an average g value of 2) for four Mn(III) ($S = 2$) and one Cr(III) ($S = 3/2$)

magnetically isolated centers. When the temperature is lowered, χT decreases gradually to reach a minimum value of ca. $11.1 \text{ cm}^3 \text{ K/mol}$ around 60 K, and then increases smoothly until 30 K before rapidly reaching a maximum value of $56.4 \text{ cm}^3 \text{ K/mol}$ at 5 K. Finally at lower temperatures, the χT product abruptly decreases to ca. $31.6 \text{ cm}^3 \text{ K/mol}$ at 1.8 K suggesting the presence of additional weaker antiferromagnetic interactions or magnetic anisotropy. Above 5 K, the thermal magnetic behavior indicates the presence of dominating antiferromagnetic interactions (J) as expected between Mn^{III} and Cr^{III} through cyanido bridges [14b,21]. Therefore the magnetic centers in the $[\{\text{Mn}(\text{saltmen})\}_4\text{Cr}(\text{CN})_6\text{]}^+$ unit are ferrimagnetically organized. Moreover, in the two-dimensional network, these pentanuclear motifs are expected to be weakly ferromagnetically coupled (J') through the out-plane double phenoxo bridges between the two adjacent Mn^{III} sites [5,6,9,16]. Considering this topology of the magnetic interactions and also that antiferromagnetic interactions

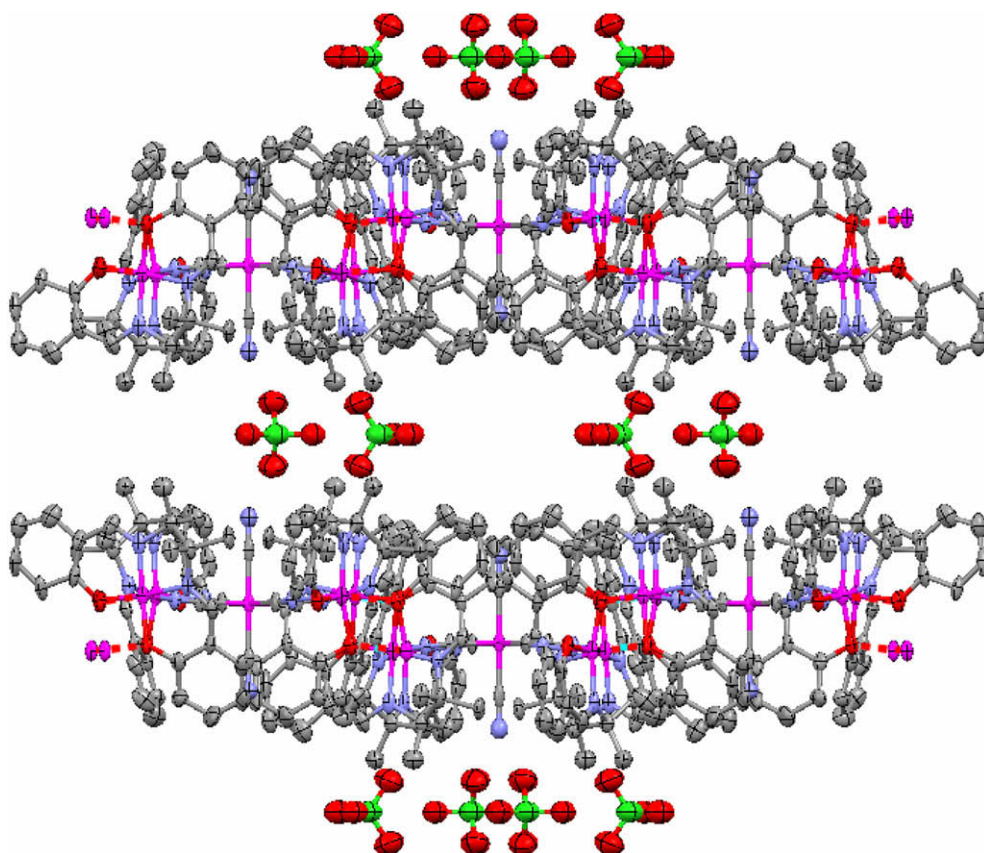


Fig. 3. view along the crystallographic a axis showing the interlayer stacking by van der Waals contact. H atoms are omitted for clarity. Colour code: Cr and Mn, purple; N, blue; C, grey; O, red; Cl, green. For interpretation of the references to colour in this figure legend, the reader is referred to the web version of this article.

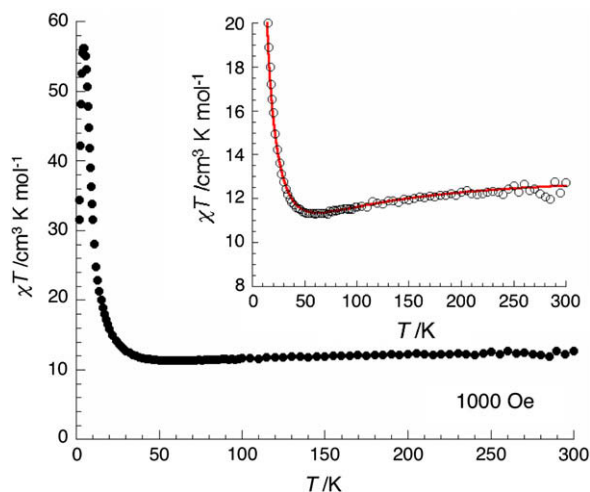


Fig. 4. Temperature dependence of χT product (with $\chi = M/H$) under an applied field of 1000 Oe. Inset: expanded view of the χT vs T plot. The red solid line represents the best simulation curve using the pentanuclear Heisenberg model described in the text. For interpretation of the references to colour in this figure legend, the reader is referred to the web version of this article.

are dominating ($|J| \gg |J'|$), an estimation of the exchange couplings has been done, simulating the thermal dependence of the magnetic susceptibility from the following isotropic Heisenberg Hamiltonian:

$$H = -2J \sum_{i=1}^4 (S_i \times S_{Cr})$$

where $S_i = S_{Mn} = 2$, $S_{Cr} = 3/2$ and J is the Mn \cdots Cr interaction via an $-NC-$ bridge. Using this model, an excellent simulation of the χT vs T data (shown in the inset of Fig. 4) has been obtained numerically using the MAGPACK program [22] and introducing inter-complex Mn^{III}–Mn^{III} interactions in mean-field approximation (J') [23].¹ The best set of parameters is $J/k_B = -7(1)$ K, $zJ'/k_B = +0.27(5)$ K and $g_{av} = 1.96$ considering only the experimental data above 14 K in the simulation, in order to avoid additional weaker antiferromagnetic interactions or magnetic anisotropy. It is worth noting that the estimation of the exchange coupling between Mn^{III} and Cr^{III} ions via the $-NC-$ linkage is slightly higher than the values usually quoted in literature ranging from -1.5 to -5 K [14b,21].

At low temperature, this coupling scheme leads to an $S_T = 13/2$ spin ground state for the $[Mn_4Cr]$ unit

¹ In order to take into account the inter-complex interaction, the following definition of the susceptibility has been used:

$$\chi = \frac{\chi_{Mn_4Cr}}{1 - \frac{2zJ'}{Ng^2\mu_B} \chi_{Mn_4Cr}}$$

see for example Ref. [23].

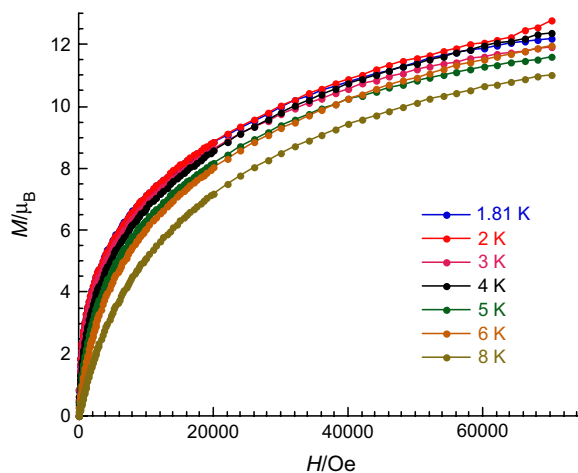


Fig. 5. Field dependence of magnetization in the field range of 0–70 000 Oe and between 1.8 and 8 K.

confirmed by the M vs H plot, at 1.8 K, shown in Fig. 5, which is almost saturated at 7 T reaching $12.6 \mu_B$. Two additional comments should be made on Fig. 5: (i) no inflection point on the M vs H plots or maximum in the dM/dH vs H plots is observed suggesting that the coupling between planes is negligible or ferromagnetic in nature; and (ii) the increase of the magnetization with the applied magnetic field is slow as expected in the presence of magnetic anisotropy. Indeed, this last remark is well in agreement with the presence of Mn(III) metal ions that usually possess magnetic anisotropy.

Interestingly, the magnetization exhibits at 1.8 K a hysteresis loop with a coercive field of about 20 Oe (Fig. 6). This behavior was still observed up to 3 K as confirmed

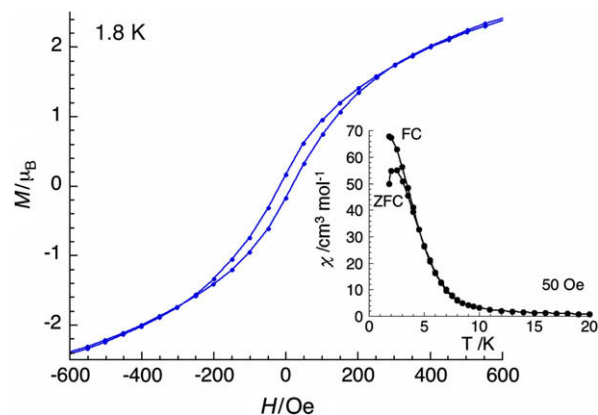


Fig. 6. Field dependence of the magnetization at low fields at 1.8 K highlighting the hysteretic behavior with a sweep-rate used in a traditional SQUID magnetometer (≈ 100 Oe/min). Inset: field-cooled (FC) magnetization and the zero-field-cooled (ZFC) magnetization vs T curves under a weak magnetic field of 50 Oe.

by the field-cooled (FC) and the zero-field-cooled (ZFC) susceptibility vs T data obtained at 50 Oe that separate around 3 K (see inset of Fig. 6).

This behavior suggests the presence of a magnetic phase transition that would be a ferrimagnetic long-range order based on the spin topology described above. In order to further investigate this magnetic behavior, ac susceptibility measurements between 1.8 and 10 K have been performed in zero dc field and 3 Oe ac field oscillating at frequencies of 1–1000 Hz. As shown in Fig. 7, the out-of-phase signals (χ'') become non-zero around 5 K independently of the ac frequency used, suggesting the occurrence of a ferrimagnetic order at $T_C = 5$ K. Nevertheless, both components of the ac susceptibility exhibit a slight frequency dependence on both the temperature of their maximum and the height of the peak. The position of the χ' and the χ'' peaks increases by ~ 0.4 K when the frequency is increased from 10 to 1000 Hz. This behavior is not expected to occur for three-dimensional “perfectly”

ordered magnets. Indeed, a shift of the peak maximum of χ' with frequency is usually indicative of a glassy magnetic phase or a superparamagnetic phase [24,25].

It is worth pointing out that we are avoiding the use of the term *spin-glass* because this term was coined for magnetically dilute systems prepared by random doping of a few atom percent of a magnetic compound into a non-magnetic, conducting host [25k]. In order to quantify the glassiness, the concept of the frequency shift γ was introduced by Mydosh who defined γ as the slope normalized at $T_f(0)$ of T_f vs $\log(\nu)$ curve where T_f is the “freezing” temperature located at the peak maximum of χ' at each frequency, $T_f(0)$ is the “freezing” temperature defined as the peak maximum of χ' extrapolated at $\log(\nu) = 0$ and $\log(\nu)$ is the logarithm of the ac frequency (ν) [24a]. In the present system, the frequency shift is estimated at 0.063 and according to Mydosh this value is consistent with glassy magnetic behavior and not with superparamagnetism for which much larger γ values (>0.1) are usually observed [24a,25a,d]. The ac susceptibility measurements reveal that this compound possesses a glassy magnetic behavior at low temperature and therefore does not undergo a “perfect” three-dimensional order. Glassiness [24] can result from two main origins (i) randomness (i.e. atom or bond disorder or defect in the crystal structure) and (ii) competing magnetic effects (i.e. interactions, anisotropy). In the present compound, both phenomena are indeed present and could be responsible for the observed glassy behavior: disorder of the ClO_4^- anions and competition between the magnetic anisotropy of the Mn(III) metal ions and the Mn(III)–Cr(III) antiferromagnetic interactions.

3.3. Magneto-structural considerations

The magneto-structural data of compound **1** can be inspected by comparison with the structurally similar previously reported MnFe systems, namely $[\{\text{Mn}(\text{saltmen})\}_4\{\text{Fe}(\text{CN})_6\}]\text{ClO}_4 \cdot \text{H}_2\text{O}$ [15] and $[\{\text{Mn}(\text{saltmen})\}_4\text{Fe}(\text{CN})_5(1 - \text{CH}_3\text{im})](\text{ClO}_4)_2 \cdot 9\text{H}_2\text{O}$ [20]. Indeed, in both cases a soft magnet is observed with, respectively, a T_C of 4.5 and 4.8 K and coercive fields of 80 and 500 Oe, which reasonably compares with the values, 5 K and 20 Oe, found here for **1**. Nevertheless in these MnFe systems, both Mn–Mn (through double saltmen phenoxo bridge) and Mn–Fe (through cyanido bridge) interactions were found to be ferromagnetic. On the other hand, the only known structurally similar MnCr system, namely $[\{\text{Mn}(\text{saltmen})\}_4\text{Cr}(\text{CN})_5(\text{NO})]\text{ClO}_4 \cdot 3\text{H}_2\text{O}$ [19], also presents the magnetic properties of a soft magnet ($T_C = 6.4$ K and $H_C = 10$ Oe) and does show

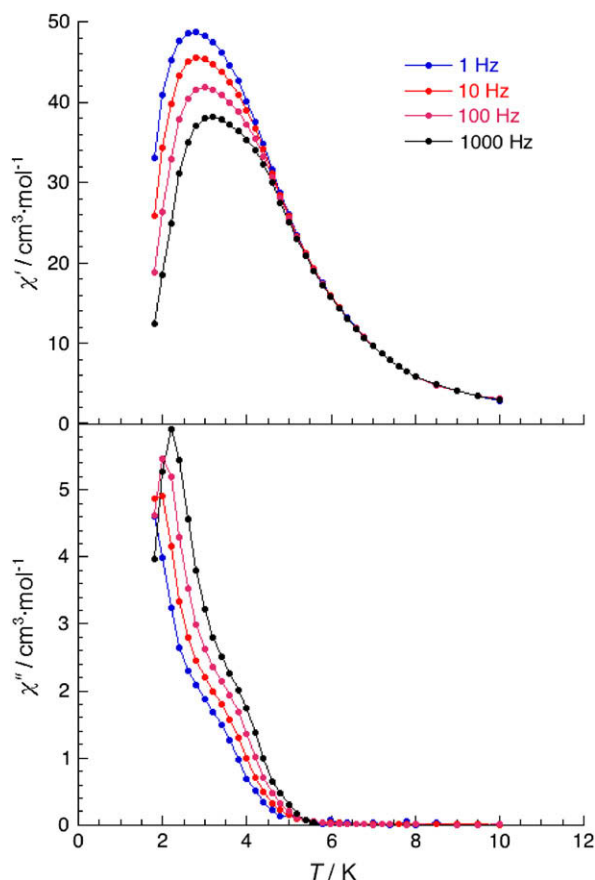


Fig. 7. Temperature dependence of the real and imaginary components of the ac susceptibility in a zero applied static field with an oscillating field of 3 Oe at frequencies of 1, 10, 100 and 1000 Hz.

antiferromagnetic interaction in its Mn–NC–Cr pairs. Ferromagnetic interaction in the Fe^{III}–CN–Mn^{III} pairs is thought to occur because bending of the Mn–N≡C moiety that results in diminishing of the orbital overlap among the metallic cations. Nevertheless, a similar bending is observed in **1** and these three related compounds, the Mn–N–C angle being, respectively, 156.2°, 156.1°, 149.8° and 154.6°. In the two MnCr systems, **1** and [Mn(saltmen)₄Cr(CN)₅(NO)]ClO₄·3H₂O, the Cr–C≡N moiety is also bent while it is linear in the MnFe ones, but the deviation from linearity is too small (the Cr–C–N angle is, respectively, 174.7° and 175.2°) to explain the change in sign of the interaction. The observations on these four 2D Mn(III)–M(III) systems actually pertain to a general trend, since most cyanide-bridged Mn(III)–Fe(III) complexes reported in the literature exhibit ferromagnetic interactions while this is not so far the case for any Mn(III)–Cr(III) complex. Simple orbital considerations, based on the model of localized orbitals developed by Kahn,² may explain these observations. Indeed, if one chooses the *z* local axis to be along the Mn and Fe or Cr–cyanido bond, then two antiferromagnetic paths corresponding to the d_{xz}–d_{xz} and d_{yz}–d_{yz} orbital overlaps occur. Nevertheless, the electronic configurations for the low spin Fe(III) that possesses only one unpaired electron on d_{xy}, d_{xz} or d_{yz} orbitals, are degenerated and therefore equally populated with a statistical factor of 1/3. On the other hand in the case of Cr(III), a single electronic configuration is possible with one unpaired electron in both d_{xz} and d_{yz} orbitals. Therefore, with similar structural parameters, the overlaps among magnetic orbitals, giving rise to the antiferromagnetic contribution, should be three times stronger for the Mn(III)–NC–Cr(III) pair than for the Mn(III)–NC–Fe(III) pair. In the latter case bending of the Mn–N≡C moiety can reduce sufficiently these overlaps to result in an overall ferromagnetic interaction, while in the former case, the antiferromagnetic contribution to the exchange coupling seems to remain dominant, in agreement with experimental data of both compound **1** and [Mn(saltmen)₄Cr(CN)₅(NO)]ClO₄·3H₂O.³

4. Conclusions

An extended 2D layered Mn(III)–Cr(III) coordination complex has been obtained through reaction of

[Cr^{III}(CN)₆]³⁻ and [Mn^{III}(saltmen)]⁺ building block sources. Its structure is based on a pentameric unit formed through four Cr(III)–CN–Mn(III) bridges, these units being connected into layers through double phenoxo Mn–O···Mn bridges. The corresponding antiferromagnetic and weak ferromagnetic exchange couplings result in a ferrimagnetic ordering at around 5 K, although some degree of glassiness has been observed. Magneto-structural comparison with similar ferromagnetically coupled Fe(III)Mn(III) systems indicates that the observed antiferromagnetic coupling in the cyanide-bridged Cr(III)Mn(III) systems is simply resulting from Cr(III) d³ electronic configuration resulting in a stronger overlap among magnetic orbitals.

Acknowledgements

This work was supported by the CNRS, the University of Bordeaux 1 and the Conseil Régional d'Aquitaine. R.C. and X.L. thank the Chinese Scholarship Council for the funding of the scientific stay of X.L. at the CRPP.

References

- [1] O. Kahn, *Molecular Magnetism*, Wiley-VCH, New York, 1991.
- [2] (a) R. Sessoli, D. Gatteschi, *Angew. Chem., Int. Ed.* 42 (2003) 268;
 - (b) G. Aromi, E.K. Brechin, *Struct. Bond.* 122 (2006) 1.
- [3] (a) S. Ferlay, T. Mallah, R. Ouahès, P. Veillet, M. Verdager, *Nature* 378 (1995) 701;
 - (b) W.R. Entley, G.S. Girolami, *Science* 268 (1995) 397.
- [4] (a) A. Caneschi, D. Gatteschi, N. Lalioti, C. Sangregorio, R. Sessoli, G. Venturi, A. Vindigni, A. Rettori, M.G. Pini, M.A. Novak, *Angew. Chem., Int. Ed.* 40 (2001) 1760;
 - (b) A. Caneschi, D. Gatteschi, N. Lalioti, C. Sangregorio, R. Sessoli, G. Venturi, A. Vindigni, A. Rettori, M.G. Pini, M.A. Novak, *Europhys. Lett.* 58 (2002) 771;
 - (c) E. Pardo, R. Ruiz-Garcia, F. Lloret, J. Faus, M. Julve, Y. Journaux, F. Delgado, C. Ruiz-Perez, *Adv. Mater.* 16 (2004) 1597;
 - (d) Z.-M. Sun, A.V. Prosvirin, H.-H. Zhao, J.-G. Mao, K.R. Dunbar, *J. Appl. Phys.* 97 (2005) 10B305;
 - (e) T. Kajiwara, M. Nakano, Y. Kaneko, S. Takaishi, T. Ito, M. Yamashita, A. Igashira-Kamiyama, H. Nojiri, Y. Ono, N. Kojima, *J. Am. Chem. Soc.* 127 (2005) 10150;
 - (f) J.P. Costes, J.M. Clemente-Juan, F. Dahan, J. Milon, *Inorg. Chem.* 43 (2004) 8200;
 - (g) L. Bogani, C. Sangregorio, R. Sessoli, D. Gatteschi, *Angew. Chem., Int. Ed.* 44 (2005) 5817;
 - (h) K. Bernot, L. Bogani, A. Caneschi, D. Gatteschi, R. Sessoli, *J. Am. Chem. Soc.* 128 (2006) 7947;
 - (i) L. Bogani, L. Cavigli, K. Bernot, R. Sessoli, M. Gurioli, D. Gatteschi, *J. Mater. Chem.* 16 (2006) 2587;
 - (j) A. Palii, S. Ostrovsky, S. Klokishner, O.S. Reu, Z.-M. Sun, A.P. Prosvirin, H.-H. Zhao, J.-G. Mao, K.R. Dunbar, *J. Phys. Chem. A* 110 (2006) 14003;

² See Ref. [1], Chapter IX.

³ Although the authors in Ref. [19] assigned the oxidation state of Cr in [Cr(CN)₅(NO)] as +1, the observed magnetic behavior point at a probable +3 oxidation state, as indeed considered by the authors in their conclusion and previously argued in M. Ardon, S. Cohen, *Inorg. Chem.* 32 (1993) 3241.

- (k) X.-T. Liu, X.-Y. Wang, W.-X. Zhang, P. Cui, S. Gao, *Adv. Mater.* 18 (2006) 2852;
- (l) X.-T. Liu, X.-Y. Wang, S. Gao, R. Cao, *Inorg. Chem.* 45 (2006) 1508;
- (m) N. Ishii, T. Ishida, T. Nogami, *Inorg. Chem.* 45 (2006) 3837;
- (n) X.-N. Cheng, W.-X. Zhang, Y.-Z. Zheng, X.-M. Chen, *Chem. Commun.* (2006) 3603;
- (o) Y.-L. Bai, J. Tao, W. Wernsdorfer, O. Sato, R.-B. Huang, L.-S. Zheng, *J. Am. Chem. Soc.* 128 (2006) 16428;
- (p) H. Miyasaka, T. Madanbashi, K. Sugimoto, Y. Nakazawa, W. Wernsdorfer, K. Sugiura, M. Yamashita, C. Coulon, R. Clérac, *Chem. Eur. J.* 12 (2006) 7028;
- (q) E. Pardo, R. Ruiz-García, F. Lloret, J. Faus, M. Julve, Y. Journaux, M.A. Novak, F. Delgado, C. Ruiz-Pérez, *Chem. Eur. J.* 13 (2007) 2054.
- [5] (a) R. Clérac, H. Miyasaka, M. Yamashita, C. Coulon, *J. Am. Chem. Soc.* 124 (2002) 12837;
- (b) H. Miyasaka, R. Clérac, K. Mizushima, K. Sugiura, M. Yamashita, W. Wernsdorfer, C. Coulon, *Inorg. Chem.* 42 (2003) 8203.
- [6] C. Coulon, H. Miyasaka, R. Clérac, *Struct. Bond.* 122 (2006) 163.
- [7] N.E. Chakov, W. Wernsdorfer, K.A. Abboud, G. Christou, *Inorg. Chem.* 43 (2004) 5919.
- [8] (a) F. Chang, S. Gao, H.-L. Sun, Y.-L. Hou, G. Su, in: *Proceeding of the ICSM 2002 Conference, Shanghai, China*, p. 182.
- (b) R. Lescouëzec, J. Vaissermann, C. Ruiz-Pérez, F. Lloret, R. Carrasco, M. Julve, M. Verdager, Y. Dromzee, D. Gatteschi, W. Wernsdorfer, *Angew. Chem., Int. Ed.* 42 (2003) 1483;
- (c) L.M. Toma, R. Lescouëzec, F. Lloret, M. Julve, J. Vaissermann, M. Verdager, *Chem. Commun.* (2003) 1850;
- (d) T.-F. Liu, D. Fu, S. Gao, Y.-Z. Zhang, H.-L. Sun, G. Su, Y.-J. Liu, *J. Am. Chem. Soc.* 125 (2003) 13976;
- (e) N. Shaikh, A. Panja, S. Goswami, P. Banerjee, P. Vojtysek, Y.-Z. Zhang, G. Su, S. Gao, *Inorg. Chem.* 43 (2004) 849;
- (f) R. Lescouëzec, L.M. Toma, J. Vaissermann, M. Verdager, F.S. Delgado, C. Ruiz-Pérez, F. Lloret, M. Julve, *Coord. Chem. Rev.* 249 (2005) 2691;
- (g) Y.-Z. Zheng, M.-L. Tong, W.-X. Zhang, X.-M. Chen, *Angew. Chem., Int. Ed.* 45 (2006) 6310;
- (h) H.-R. Wen, C.-F. Wang, Y. Song, S. Gao, J.-L. Zuo, X.-Z. You, *Inorg. Chem.* 45 (2006) 8942;
- (i) L.M. Toma, R. Lescouëzec, J. Pasan, C. Ruiz-Pérez, J. Vaissermann, J. Cano, R. Carrasco, W. Wernsdorfer, F. Lloret, M. Julve, *J. Am. Chem. Soc.* 128 (2006) 4842;
- (j) A. Saitoh, H. Miyasaka, M. Yamashita, R. Clérac, *J. Mater. Chem.* 17 (2007) 2002.
- [9] H. Miyasaka, R. Clérac, *Bull. Chem. Soc. Jpn.* 78 (2005) 1725.
- [10] M. Ohba, N. Usuki, N. Fukita, H. Okawa, *Angew. Chem., Int. Ed.* 38 (1999) 1795.
- [11] C.P. Berlinguette, D. Vaughn, C. Cañada-Vilalta, J.R. Galán-Mascarós, K.R. Dunbar, *Angew. Chem., Int. Ed.* 42 (2003) 1523.
- [12] (a) D. Li, R. Clérac, O. Roubeau, E. Harté, C. Mathonière, R. Le Bris, S.M. Holmes, *J. Am. Chem. Soc.* 130 (2008) 252;
- (b) O. Sato, Y. Einaga, A. Fujishima, K. Hashimoto, *Inorg. Chem.* 38 (1999) 4405;
- (c) A. Goujon, O. Roubeau, F. Varret, A. Dolbecq, A. Bleuzen, M. Verdager, *Eur. Phys. J. B* 14 (2000) 115;
- (d) C.C. dit Moulin, F. Villain, A. Bleuzen, M.A. Arrio, P. Sainctavit, C. Lomenech, V. Escax, F. Baudelet, E. Dartyge, J.J. Gallet, M. Verdager, *J. Am. Chem. Soc.* 122 (2000) 6653.
- [13] (a) C. Kachi-Terajima, H. Miyasaka, A. Saitoh, N. Shirakawa, M. Yamashita, R. Clérac, *Inorg. Chem.* 46 (2007) 5861;
- (b) H. Miyasaka, T. Nezu, K. Sugimoto, K. Sugiura, M. Yamashita, R. Clérac, *Chem. Eur. J.* 11 (2005) 1592;
- (c) L. Lecren, W. Wernsdorfer, Y.-G. Li, A. Vindigni, H. Miyasaka, R. Clérac, *J. Am. Chem. Soc.* 129 (2007) 5045.
- [14] (a) H.J. Choi, J.J. Sokol, J.R. Long, *J. Phys. Chem. Solids* 65 (2004) 839;
- (b) H.J. Choi, J.J. Sokol, J.R. Long, *Inorg. Chem.* 43 (2004) 1606;
- (c) S.F. Si, J.K. Tang, Z.Q. Liu, D.Z. Liao, Z.H. Jiang, S.P. Yan, P. Cheng, *Inorg. Chem. Commun.* 6 (2003) 1109.
- [15] (a) H. Miyasaka, N. Matsumoto, H. Okawa, N. Re, E. Gallo, C. Floriani, *J. Am. Chem. Soc.* 118 (1996) 981;
- (b) H. Miyasaka, N. Matsumoto, N. Re, E. Gallo, C. Floriani, *Inorg. Chem.* 36 (1997) 670.
- [16] H. Miyasaka, R. Clérac, T. Ishii, H.C. Chang, S. Kitagawa, M. Yamashita, *J. Chem. Soc., Dalton Trans.* (2002) 1528.
- [17] Z. Otwinowski, W. Minor, *Methods Enzymol.* 276 (1996) 307.
- [18] (a) G.M. Sheldrick, SHELXL97, Program for Crystal Structure Refinement, University of Göttingen, Göttingen, Germany, 1997;
- (b) G.M. Sheldrick, SHELXS97, Program for Crystal Structure Solution, University of Göttingen, Göttingen, Germany, 1997.
- [19] Z.H. Ni, L. Zheng, L.F. Zhang, A.L. Cui, W.W. Ni, C.C. Zhao, H.Z. Kou, *Eur. J. Inorg. Chem.* (2007) 1240.
- [20] W.W. Ni, Z.H. Ni, A.L. Cui, X. Liang, H.Z. Kou, *Inorg. Chem.* 46 (2007) 22.
- [21] (a) X. Shen, B. Li, J. Zou, Z. Xu, Y. Yu, S. Liu, *Trans. Met. Chem.* 27 (2002) 372;
- (c) H. Miyasaka, H. Takahashi, T. Madanbashi, K.-I. Sugiura, R. Clérac, H. Nojiri, *Inorg. Chem.* 44 (2005) 5969.
- [22] J.J. Borrás-Almenar, J.M. Clemente-Juan, E. Coronado, B.S. Tsukerblat, *J. Comput. Chem.* 22 (2001) 985.
- [23] (a) B.E. Myers, L. Berger, S. Friedberg, *J. Appl. Phys.* 40 (1969) 1149;
- (b) C.J. O'Connor, *Prog. Inorg. Chem.* 29 (1982) 203.
- [24] (a) J.A. Mydosh, *Spin Glasses: An Experimental Introduction*, Taylor & Francis, London, 1993, p. 64;
- (b) D. Chowdhury, *Spin Glasses and Other Frustrated Systems*, Princeton University Press, New Jersey, 1986;
- (c) K. Moorjani, J.M.D. Coey, *Magnetic Glasses*, Elsevier, Amsterdam, 1984;
- (d) K. Binder, A.P. Young, *Rev. Mod. Phys.* 58 (4) (1986) 801;
- (e) C.J. O'Connor, *Research Frontiers in Magnetochemistry*, in: C.J. O'Connor (Ed.), World Scientific, London, 1993, p. 109;
- (f) A.P. Ramirez, *Annu. Rev. Mater. Sci.* 24 (1994) 453.
- [25] (a) R.D. Sommer, B.J. Korte, S.P. Sellers, G.T. Yee, *Mater. Res. Soc. Symp. Proc.* 488 (1998) 471;
- (b) S.P. Sellers, B.B. Korte, J.P. Fitzgerald, W.M. Reiff, G.T. Yee, *J. Am. Chem. Soc.* 120 (19) (1998) 4662;
- (c) B.B. Kaul, W.S. Durfee, G.T. Yee, *J. Am. Chem. Soc.* 121 (1999) 6862;
- (d) W.E. Bushmann, J. Ensling, P. Gütlich, J.S. Miller, *Chem. Eur. J.* 5 (10) (1999) 3019;
- (e) C.M. Wynn, A.S. Albrecht, C.P. Landee, C. Navas, M.M. Turnbull, *Mol. Cryst. Liq. Cryst. Sci. Technol., Sect. A* 274 (1995) 657;
- (f) C.P. Landee, C.M. Wynn, A.S. Albrecht, W. Zhang, G.B. Vunni, J.L. Parent, C. Navas, M.M. Turnbull, *J. Appl. Phys.* 75 (1994) 5535;

(g) W.E. Buschmann, J.S. Miller, *Inorg. Chem.* 39 (2000) 2411;
(h) E.J. Brandon, D.K. Rittenberg, A.M. Arif, J.S. Miller, *Inorg. Chem.* 37 (1998) 3376;
(i) E.J. Brandon, A.M. Arif, B.M. Burkhart, J.S. Miller, *Inorg. Chem.* 37 (1998) 2792;

(j) R.J. Cava, A.P. Ramirez, Q. Huang, J.J. Krajewski, *J. Solid State Chem.* 140 (1998) 337;
(k) R. Clérac, S. O’Kane, J. Cowen, X. Ouyang, R. Heintz, H. Zhao, M.J. Bazile Jr., K.R. Dunbar, *Chem. Mater.* 15 (2003) 1840.